Prostaglandin-E2 Receptor-4 Stimulant Rescues Cardiac Malfunction during Myocarditis and Protects the Heart from Adverse Ventricular Remodeling after Myocarditis

Akira Takakuma
Yokohama City University Graduate School of Medicine
Mototsugu Nishii (s461211@yokohama-cu.ac.jp)
Yokohama City University Graduate School of Medicine
Alan Valaperti
University Hospital Zurich
Haruto Hiraga
Yokohama City University Graduate School of Medicine
Ryo Saji
Yokohama City University Graduate School of Medicine
Kazuya Sakai
Yokohama City University Graduate School of Medicine
Reo Matsumura
Yokohama City University Graduate School of Medicine
Yasuo Miyata
Yokohama City University Graduate School of Medicine
Nozomu Oba
Yokohama City University Graduate School of Medicine
Fumiya Nunose
Yokohama City University Graduate School of Medicine
Fumihiro Ogawa
Yokohama City University Graduate School of Medicine
Kouichi Tamura
Yokohama City University
Ichiro Takeuchi
Yokohama City University Graduate School of Medicine

Research Article

Keywords: Prostaglandin-E2, Receptor-4, Cardiac Malfunction, Myocarditis , Ventricular Remodeling

Posted Date: August 10th, 2021

DOI: https://doi.org/10.21203/rs.3.rs-775642/v1

Abstract

Cardioprotective effect of prostaglandin-E2 receptor-4 (EP4) stimulation on the ischemic heart has been demonstrated. Its effect on the heart affected by myocarditis, however, remains uncertain. In this study, we investigated therapeutic effect of EP4 stimulant using a mouse model of autoimmune myocarditis (EAM) that progresses to dilated cardiomyopathy (DCM). EP4 was present in the hearts of EAM mice. Treatment with EP4 agonist (ONO-0260164: 20 mg/kg/day) improved an impaired left ventricular (LV) contractility and reduction of blood pressure on day 21, a peak myocardial inflammation. Alternatively, DCM phenotype, characterized by LV dilation, LV systolic dysfunction, and collagen deposition, without inflammatory profiles was observed on day 56, along with activation of matrix metalloproteinase (MMP) 2 critical for myocardial extracellular matrix disruption, indicating an important molecular mechanism underlying adverse ventricular remodeling after myocarditis. Continued treatment with ONO-0260164 alleviated the DCM phenotype, but this effect was counteracted by its combination with a EP4 antagonist. Moreover, ONO-0260164 inhibited *in vivo* proteolytic activity of MMP2 in association with up-regulation of tissue inhibitor of metalloproteinase (TIMP)-3. EP4 stimulant may be a promising and novel therapeutic agent that rescues cardiac malfunction during myocarditis and prevents adverse ventricular remodeling after myocarditis by promoting the TIMP3/MMP2 axis.

Introduction

Myocarditis is an inflammatory heart disease characterized by broad range of clinical course from cardiac malfunction requiring inotropic drugs and/or mechanical circulatory support to dilated cardiomyopathy (DCM) requiring heart transplantation.[1–2] Pharmacological treatments for inflammatory heart disease, however, have yet to be established.

Apart from chronic viral infection [3], immunohistochemical evidence and the presence of autoantibodies against myocardial structure have showed that autoimmune response, which follows the myocardial damage provoked by the initial viral infection, plays a crucial role in the pathogenesis of myocarditis and subsequent DCM.[4–5] DCM pathology is also characterized by adverse ventricular remodeling that manifests as left ventricular (LV) dilation, impaired LV contractility, and fibrosis. Disruption of myocardial extracellular matrix (ECM), that provides myocardial wall mechanics, by matrix metalloproteinases (MMPs) activation [6] critically provokes adverse ventricular remodeling.[7] Cardiac fibrosis characterized by accumulation of collagen deposit in the myocardial interstitium [8] also results in profound impairment of LV systolic and diastolic function via disrupting the coordination of myocardial excitation-contraction coupling in both systole and diastole.[9–10]

Prostaglandin (PG) E2 (PGE2) has been implicated in the pathogenesis of inflammatory diseases through four specific receptors (EP 1–4 receptors).[11] Particularly, functional and morphological analyses using genetic modification and selective agonist and antagonist have shown that EP4 receptor stimulation protects the heart from cardiac rupture and improves cardiac function after ischemia-reperfusion injury

[12–14] and further alleviates cardiac fibrosis in pressure-overloaded heart.[15] Its effect on the heart affected by myocarditis, however, remains elusive.

The BALB/c mouse model of experimental autoimmune myocarditis (EAM) allows to study not only autoimmune mechanisms, but also transition from myocarditis to DCM.[16] In the present study, we investigated the molecular mechanisms underlying adverse ventricular remodeling caused by myocarditis and related therapeutic effect of EP4 receptor stimulant using a mouse EAM model and showed for the first time that EP4 stimulant protects the heart from adverse ventricular remodeling after myocarditis by controlling myocardial ECM metabolism.

Results

EP4 receptor expression in EAM

Immunoblot in bulk heart tissue showed that EP4 receptor is present in the hearts of EAM mice (Supplementary Fig. 1A). Moreover, immunostaining at 21 days after immunization, when myocardial inflammation was at its peak, showed expression of EP4 receptor in myocytes and infiltrating cells at the inflamed site (Supplementary Fig. 1B).

Effects of a EP4 receptor selective agonist in healthy mice.

To identify optimal dose of ONO-0260164, a EP4 receptor selective agonist for *in vivo* study, systolic blood pressure (BP), body weight (BW), and echocardiographic parameters were evaluated in healthy mice treated with ONO-0260164. The BP was significantly decreased 1 or 2 hours after a single administration of ONO-0260164 (20 or 50 mg/kg) compared with before the administration, although the heart rate (HR) did not change between before and after the administration (Supplementary Fig. 2A). Conversely, daily administration of ONO-0260164 (20 or 50 mg/kg/day) significantly reduced HR but had no effect on BP (Supplementary Fig. 2B). Alternatively, the BW was significantly increased in the 50 mg/kg/day group of ONO-0260164 compared to the vehicle only group, but not in 2 or 20 mg/kg/day group. The change in BW from day 21 to day 49 also followed the same manner (Supplementary Fig. 2C).

Daily administration of ONO-0260164 did not affect echocardiographic parameters on day 21, including LV end-diastolic dimension (LVDd), LV end-systolic dimension (LVDs), interventricular septum diastolic thickness (IVSd), LV posterior wall diastolic thickness (PWd), LV fractional shortening (FS), and LV mass index (LVMI) (Supplementary Fig. 3A). However, LVMI as well as IVSd and PWd on day 49 was significantly increased in the 50 mg/kg/day group of ONO-0260164 compared to the vehicle only group, but not in the 20 mg/kg/day group of ONO-0260164 (Supplementary Fig. 3B). Therefore, we decided to use 20 mg/kg/day of ONO-0260164 for *in vivo* investigation.

Immunomodulation by EP4 receptor signaling in acute EAM.

In contrast to a previous report showing the anti-inflammatory effect of a selective EP4 receptor agonist on acute EAM [17], daily treatment with CJ-42794, a selective EP4 antagonist, from day 14 to day 21, significantly exacerbated myocardial inflammation on day 21 compared to vehicle alone (inflamed area: 7.2 ± 1.4 % vs. 2.0 ± 0.8 %, P = 0.0202; macroscopic score: 2.4 ± 0.2 vs. 1.6 ± 0.2, P = 0.0067; respectively) (Fig. 1A, B). Consistently, cardiac protein expression of the EAM inducible Th17-specific master transcription factor, retinoic acid receptor-related orphan nuclear receptor (ROR γt) [18] on day 21 was significantly increased in CJ-42794-treated EAM compared with in vehicle-treated EAM (The ratio of ROR γt to GAPDH: 2.0 ± 0.6 vs. 0.2 ± 0.1, P = 0.0450, respectively) (Fig. 1C, D).

These observations suggest that EP4 receptor stimulation modulates the development of myocardial inflammation.

Blood pressure in acute EAM mice and its control by EP4 receptor stimulation.

There was no significant difference of the HR on day 21 between CJ-42794-treated EAM and vehicle alone-treated EAM (603 ± 17 bpm vs, 587 ± 12 bpm, P = 0.4725, respectively), while BP was significantly decreased in the EAM treated with CJ-42794 compared with in the EAM treated with vehicle (106 ± 2 mmHg vs. 119 ± 3 mmHg, P = 0.0090; respectively) (Fig. 2A). Conversely, significant reduction of BP on day 21 in EAM (EAM vs. non-EAM: 98 ± 3 mmHg vs. 113 ± 3 mmHg, P = 0.0303, respectively) was improved by treatment with ONO-0260164 (113 ± 3 mmHg, P = 0.0030). The HR on day 21 was significantly decreased in the ONO-0260164-treated EAM compared to the vehicle alone-treated EAM (574 ± 23 bpm vs. 666 ± 17 bpm, P = 0.0085, respectively) (Fig. 2B).

These results suggest that EP4 receptor stimulation positively affects the BP during myocarditis.

Cardiac malfunction in acute phase of EAM mice and its control by EP4 receptor stimulation.

Cardiac function was evaluated with echocardiography on day 21. LVFS and LV dimensions were significantly reduced and increased, respectively in CJ-42794-treated EAM compared to vehicle-treated EAM (LVFS: 60 ± 2 % vs. 67 ± 2 %, P = 0.0472; LVDd: 3.1 ± 0.1 mm vs. 2.7 ± 0.1 mm, P = 0.0236; LVDs: 1.2 ± 0.1 mm vs. 0.9 ± 0.1 mm, P = 0.0350; respectively) (Fig. 3A). Conversely, impairment of LV contractility and LV dilation in EAM (EAM vs. non-EAM: [LVFS] 40 ± 4 % vs. 77 ± 1 %, P < 0.0001; [LV posterior wall systolic thickness: PWs] 1.4 ± 0.1 mm vs. 1.8 ± 0.1 mm, P = 0.0136; [LVDs] 1.9 ± 0.3 mm vs. 0.5 ± 0.1 mm, P = 0.0006; [LVDd] 3.1 ± 0.2 mm vs. 2.5 ± 0.1 mm, P = 0.0373; respectively) were alleviated by daily

treatment with ONO-0260164 (LVFS: 69 ± 3 %, P < 0.0001; PWs: 1.7 ± 0.1 mm, P = 0.0348; LVDs: 0.7 ± 0.1 mm, P = 0.0007; LVDd: 2.2 ± 0.1 mm, P = 0.0002) (Fig. 3B and Supplementary Video 1). We next tested if co-treatment with CJ-42794 enable to negate the effects of ONO-0260164. Impairment of LV contractility and LV dilation in EAM (EAM vs. non-EAM: [LVFS] 46.6 ± 4.8 % vs. 76.5 ± 0.8 %, P = 0.0003; [LVDd] 2.9 ± 0.1 mm vs. 2.5 ± 0.1 mm, P = 0.1294; [LVDs] 1.6 ± 0.2 mm vs. 0.5 ± 0.04 mm, P = 0.0028; respectively) were improved by treatment with ONO-0260164 (LVFS: 62.2 ± 3.5 %, P = 0.0491: LVDd: 2.4 ± 0.1 mm, P = 0.0180; LVDs: 0.9 ± 0.1 mm, P = 0.0340), but this improvement was not seen in co-treatment with CJ-42794 (LVFS: 49.7 ± 5.1 %, P = 0.9537; LVDd: 2.9 ± 0.2 mm, P = 0.9997; LVDs: 1.5 ± 0.2 mm, P = 0.9993; vs. vehicle alone-treated EAM) (Fig. 3C).

These results suggest that treatment with ONO-0260164 improves cardiac malfunction during myocarditis via EP4 receptor stimulation.

DCM phenotype in late phase of EAM mice and its prevention by EP4 receptor stimulation.

DCM phenotype characterized by impairment of LV contractility and LV dilation was evaluated with echocardiography on day 56. DCM phenotype persisted in the late phase of EAM (EAM vs. non-EAM: [LVFS] 37.4 ± 5.2 % vs. 72.4 ± 2.4 %, P = 0.0002; [PWs] 1.4 ± 0.1 mm vs. 1.7 ± 0.04 mm, P = 0.0156; [interventricular septum systolic thickness: IVSs] 1.6 ± 0.1 mm vs. 2.0 ± 0.03 mm, P = 0.0257; [LVDs] 2.1 ± 0.39 mm vs. 0.7 ± 0.03 mm, P = 0.0105; [LVDd] 3.2 ± 0.29 mm vs. 2.6 ± 0.05 mm, P = 0.0368; respectively). However, its persistence was inhibited by continued treatment with ONO-0260164 (LVFS: 62.6 ± 4.0 %, P = 0.0018; PWs: 1.6 ± 0.1 mm, P = 0.0313; IVSs: 2.0 ± 0.07 mm, P = 0.0331; LVDs: 0.9 ± 0.12 mm, P = 0.0157; LVDd: 2.3 ± 0.07 mm, P = 0.0008). Moreover, these parameters did not show significant differences between ONO-0260164-treated EAM and non-EAM (LVFS: P = 0.3405; PWs: P = 0.8301; IVSs: P = 0.8905; LVDs: P = 0.8870; LVDd: P = 0.4137), suggesting that continued treatment with ONO-0260164 completely suppressed LV remodeling after myocarditis (Fig. 4A and Supplementary Video 2). We tested if co-treatment with CJ-42794 enable to negate the cardioprotective effect of ONO-0260164. DCM phenotype in the late EAM (EAM vs. non-EAM: [LVFS] 47.5 ± 4.0 % vs, 68.0 ± 2.3 %, P = 0.0115; [IVSs] 1.6 ± 0.13 mm vs. 2.0 ± 0.03 mm, P = 0.0267; [LVDs] 1.6 ± 0.15 mm vs. 0.8 ± 0.05 mm, P = 0.0181; [LVDd] 3.0 ± 0.05 mm vs. 2.6 ± 0.02 mm, P = 0.0490; respectively) were significantly inhibited by ONO-0260164 administration (LVFS: 64.8 ± 2.9 %, P = 0.0166; IVSs: 2.0 ± 0.07 mm, P = 0.0349; LVDs: 0.8 ± 0.07 mm, P = 0.0132; LVDd: 2.4 ± 0.07 mm, P = 0.0004; respectively), but the effect was lost when combined with CJ-42794 (LVFS: 52.0 ± 5.9 %, P = 0.8523; IVSs 1.7 ± 0.08 mm, P = 0.8616; LVDs: 1.5 ± 0.29 mm, P = 0.9979; LVDd: 3.1 ± 0.18 mm, P = 0.8302; vs. vehicle alone-treated EAM) (Fig. 4B). Alternatively, the late EAM mice had no significant reduction of BP compared to non-EAM mice, and continued treatment with ONO-0260164 did not affect the BP in the late EAM (non-EAM vs. vehicle alone-treated EAM vs. ONO-0260164-treated EAM: 115 ± 3 mmHg vs. 122 ± 2 mmHg vs. 120 ± 3 mmHg, respectively; ANOVA P = 0.8914) (Fig. 4C).

Collectively, continued treatment with ONO-0260164 prevented the development of DCM phenotype after myocarditis via EP4 receptor stimulation, without affecting blood pressure.

Myocardial collagen deposition in late phase of EAM mice and its control by EP4 receptor stimulation.

Accumulation of ECM including fibrillar collagen in the myocardial interstitium is the hallmark of cardiac fibrosis [8] that greatly contributes to the development of DCM.[19] EAM mice histologically had more extensive deposition of myocardial collagen on day 56, together with larger LV cavity, compared to non-EAM mice (collagen deposition area: 24.7 ± 3.0 % vs. 0.7 ± 0.1 %, P < 0.0001, respectively), while the deposition was reduced by the treatment with ONO-0260164 (collagen deposition area: 12.3 ± 2.4 %, P = 0.0033). Moreover, this reduction was abrogated by pharmacological blockade of EP4 receptor with CJ-42794, as shown by the lack of significant difference of collagen deposition area between vehicle alone-treated EAM and both ONO-0260164 and CJ-42794-treated EAM (20.3 ± 2.7 %, P = 0.5994, respectively) (Fig. 5A, B).

We next evaluated cardiac gene expression of collagen type I, alpha 1 (Col1a1) and type III, alpha 1 (Col3a1) on day 56. Significantly increased their expression in the late EAM compared to non-EAM (Col1a1: 1.9 ± 0.26 vs. 1.0 ± 0.03, P = 0.0426; Col3a1: 3.7 ± 0.67 vs. 1.0 ± 0.02, P = 0.0008; respectively) was reduced by more than 50% when EAM was continuously treated with ONO-0260164 (Col1a1: 0.9 ± 0.12, P = 0.0259; Col3a1: 1.5 ± 0.22, P = 0.0046; vs. vehicle alone-treated EAM). However, the significant reduction was reversed by co-treatment with CJ-42794 (Col1a1: 2.0 ± 0.24, P = 0.0051; Col3a1: 3.0 ± 0.28, P = 0.0394; vs. ONO-0260164-treated EAM) (Fig. 5C).

Collectively, continued treatment with ONO-0260164 inhibited type I and type III collagen production and alleviated myocardial collagen deposition after myocarditis via EP4 receptor stimulation.

The MMP2 activation after myocarditis and its inhibition by EP4 receptor stimulant.

Disruption of myocardial ECM via MMPs including MMP2 and MMP9 is a key trigger of adverse ventricular remodeling [20–23], which is an important pathogenesis of DCM. To elucidate the molecular mechanisms underlying the development of DCM after myocarditis, we evaluated the expression and activation of MMP2 and MMP9 in the bulk heart tissues on day 56. MMP2 gene expression was increased in EAM (EAM vs. non-EAM: 1.9 ± 0.14 vs. 1.0 ± 0.06, P < 0.0001, respectively), but its increase was inhibited by treatment with ONO-0260164 (1.0 ± 0.06, P < 0.0001 vs. vehicle alone-treated EAM). On the other hand, MMP9 gene expression did not show any significant differences among non-EAM, vehicle-treated EAM, and ONO-0260164-treated EAM (Fig. 6A). Moreover, gelatin zymography showed that pro-MMP2 was significantly activated in the late EAM heart compared to non-EAM heart (The ratio of active

MMP2 to pro-MMP2: 0.0540 ± 0.0040 vs. 0.0004 ± 0.0002, P < 0.0001, respectively), while the activation of pro-MMP2 was inhibited by continued treatment with ONO-0260164 (0.0003 ± 0.0002, P < 0.0001 vs. vehicle alone-treated EAM) (Fig. 6B, C). Active MMP9 was not detected in the late EAM heart (Fig. 6B).

Collectively, myocardial ECM metabolism via MMP2 activation was associated with adverse ventricular remodeling after myocarditis, while continued treatment with ONO-0260164 attenuated transcriptional and post-transcriptional activation of MMP2.

Inflammatory and hormonal profiles in late phase of EAM mice.

We next sought molecular mechanisms of MMP2 activation after myocarditis. Inflammatory response strongly elicits MMPs activation in the process of ventricular remodeling.[6] Consistent with the echocardiographic data, EAM mice histologically had larger LV cavity on day 56 compared with that of non-EAM or ONO-0260164-treated EAM. However, myocardial inflammation was confined to small and localized areas on day 56 (Supplementary Fig. 4A) and had no significant difference between vehicle alone-treated EAM and ONO-0260164-treated EAM (Inflamed area: 0.82 ± 0.07% vs. 0.76 ± 0.16%, P = 0.6310; respectively) (Supplementary Fig. 4B). Among co-stimulatory molecules related to activated antigen presenting cells such as CD80, CD86, and CD40 and inflammatory cytokines such as interleukin (IL)-1β, tumor necrosis factor (TNF)-α, interferon (IFN)-γ, and transforming growth factor (TGF)-β1 on day 56, cardiac expression of CD40 gene was significantly yet only slightly increased in EAM compared with non-EAM (1.4 ± 0.32 vs. 1.04 ± 0.03, P = 0.0051), but did not show any significant difference between vehicle only-treated EAM and ONO-0260164-treated EAM (1.3 ± 0.21, P = 0.9042 vs. vehicle-treated EAM). Moreover, cardiac gene expression of IFN-γ and TGF-β1 was rather significantly decreased in EAM compared to non-EAM (IFN-γ: 0.27 ± 0.13 vs. 1.00 ± 0.07, P = 0.0022; TGF-β1: 0.52 ± 0.03 vs. 1.00 ± 0.04, P < 0.0001; respectively), and treatment with ONO-0260164 did not affect their gene expression in EAM mice (IFN-γ: 0.22 ± 0.06, P = 0.8994; TGF-β1: 0.58 ± 0.05, P = 0.4539; vs. vehicle-treated EAM). Other co-stimulatory molecules and pro-inflammatory cytokines had no significant difference among non-EAM, vehicle-treated EAM, and ONO-0260164-treated EAM (Supplementary Fig. 4C).

Balancing angiotensin-converting enzymes (ACE and ACE2), which controls the production of angiotensin II, is critical for the suppression of adverse ventricular remodeling, [24–26] and has been implicated in MMP2 activation.[27–28] Cardiac expression of ACE on day 56 did not show any significant difference among non-EAM, vehicle alone-treated EAM, and ONO-0260164-treated EAM (1.0 ± 0.08 vs. 1.1 ± 0.15 vs. 0.9 ± 0.16; ANOVA P = 1.1319; respectively) (Supplementary Fig. 5A), while ACE2 expression and a ratio of ACE to ACE2 were significantly decreased and increased, respectively in vehicle alone-treated EAM heart compared to non-EAM heart (ACE2: 0.27 ± 0.02 vs. 1.04 ± 0.08, P < 0.0001; a ratio of ACE to ACE2: 4.19 ± 0.62 vs. 1.00 ± 0.14, P = 0.0004; respectively) (Supplementary Fig. 5B, C, respectively). However, treatment with ONO-0260164 did not affect them in the late EAM heart (ACE2: 0.23 ± 0.01, P = 0.8311; a ratio of ACE to ACE2: 4.10 ± 0.73, P = 0.3081; vs. vehicle-treated EAM) (Supplementary Fig. 5B, C, respectively).

Collectively, an imbalance between ACE and ACE2 due to ACE2 depression could explain the MMP2 activation after myocarditis. However, treatment with ONO-0260164 had no direct effect on this imbalance.

Positive regulation of TIMP3 in the heart after myocarditis by EP4 receptor stimulant.

We evaluated the molecular mechanism by which treatment with ONO-0260164 inhibits MMP2 activation. Cardiac gene expression of membrane type 1 MMP (MT1-MMP), which is a critical endogenous activator of pro-MMP2 [29], was significantly increased in EAM (EAM vs. non-EAM: 1.80 ± 0.09 vs. 1.01 ± 0.06, P = 0.0004, respectively), while its increase was significantly mitigated by treatment with ONO-0260164 (1.36 ± 0.13, P = 0.0231, vs. vehicle alone-treated EAM) (Fig. 7A). Moreover, among endogenous tissue inhibitors of metalloproteinases (TIMPs), which consist of four sub-types: TIMP-1, TIMP-2, TIMP-3, and TIMP-4 [30], cardiac expression of TIMP2 gene was significantly and slightly decreased in EAM compared to non-EAM (0.69 ± 0.06 vs. 1.01 ± 0.06, P = 0.0042, respectively), and its expression was further reduced by treatment with ONO-0260164 (0.44 ± 0.04, P = 0.0133, vs. vehicle alone-treated EAM). In contrast to other TIMPs, TIMP2 cooperates with MT1-MMP to positively regulate the activation of pro-MMP2.[29] Cardiac gene expression of TIMP3 and − 4 was significantly reduced in EAM compared to non-EAM (TIMP3: 0.45 ± 0.11 vs. 1.00 ± 0.01, P = 0.0293; TIMP4: 0.19 ± 0.04 vs. 1.01 ± 0.06, P < 0.0001; respectively). However, their expression was increased approximately 2-fold by treatment with ONO-0260164 (TIMP3: 1.03 ± 0.18, P = 0.0164; TIMP4: 0.39 ± 0.01, P = 0.0103; vs. vehicle alone-treated EAM). Particularly, gene expression of TIMP3 in EAM restored to an equal level to non-EAM by treatment with ONO-0260164 (non-EAM vs. ONO-0260164-treated EAM: P = 0.9869) (Fig. 7B). Protein expression of TIMP3 in the heart also followed the same manner (vehicle-treated EAM vs. non-EAM: 0.02 ± 0.003 vs. 0.17 ± 0.02, P < 0.0001, respectively; ONO-0260164-treated EAM: 0.11 ± 0.02, P = 0.0008 vs. vehicle-treated EAM) (Fig. 7C, D).

Collectively, treatment with ONO-0260164 attenuated the reduction of TIMP3 in the heart after myocarditis, contributing to the control of MMP2 aberrant activation.

Discussion

MMPs play an important role in the progression of ventricular remodeling via the degradation of myocardial ECM [31] and synthesis of new collagen in the heart.[32] In a viral myocarditis model using BALB/c mice, MMP-3 and − 9 were activated in response to inflammatory responses such as IL-1β, TNF-α, and TGF-β, resulting in the development of inflammatory DCM with chronic myocarditis.[6] On the other hand, our study using an autoimmune myocarditis model in BALB/c mice showed that MMP2, but not MMP9, is activated in the pathogenesis of DCM after resolution of myocarditis, consistent with a observation in human DCM without myocarditis.[33] MMP-9 is inducibly expressed in neutrophils and

macrophages under inflammatory conditions [34], whereas MMP-2 is constitutively expressed in the myocardium.[35] This difference also supported a predominant activation of MMP2 even after resolution of myocarditis. In contrast to ACE inhibition [27], ACE2 deficiency has been shown to increase activation of MMP2 and promote adverse LV remodeling in the heart affected by myocardial infarction.[28] However, expression of ACE2 in the heart affected by myocarditis and its pathological role remained uncertain. We found that cardiac expression of ACE2, but not ACE, is reduced in the heart from the late EAM. These observations highlight that MMP2 activation associated with an imbalance between ACE and ACE2 due to reduction of ACE2 may be an important and novel molecular mechanism underlying persistent ventricular remodeling after myocarditis.

To our knowledge, there is no report defining therapeutic effect of EP4 receptor stimulant on inflammatory heart disease. Our data from the mouse EAM model showed for the first time that continued treatment with EP4 stimulant ameliorates cardiac malfunction caused by myocarditis and protects the heart affected by myocarditis from adverse ventricular remodeling.

EP4 signaling has been shown to have dual immune functions in experimental autoimmune encephalomyelitis, facilitating Th17 cell generation in peripheral lymph node during immunization, while attenuating invasion of these cells into the brain.[36–37] We found that pharmacological blockade of the EP4 receptor increases the protein expression of RORγt, a EAM inducible Th17-specific transcription factor[18] in the heart from EAM mice. This fact would imply that EP4 receptor stimulation inhibits the infiltration of Th17 T cells into the myocardium, contributing to improvement of cardiac malfunction caused by myocarditis.

Treatment with ONO-0260164 did not affect the imbalance between ACE and ACE2 but inhibited MMP2 activation in the heart after myocarditis. Alternatively, our data showed that this treatment influences gene expression of MT1-MMP and TIMPs-3/4, which tightly and strongly control MMP2 activation.[29–30] Particularly, although the association of EP4 with TIMP3 has not been elucidated, we found that treatment with ONO-0260164 reversed the EAM-induced decrease in protein and gene levels of TIMP3 in the heart to baseline levels. So far, the causal roles of MT1-MMP and TIMPs-3/4 in the progression of myocardial disease have been demonstrated.[38–40] Based on these findings, stimulating EP4 receptors to suppress MMP2 expression and positively regulating TIMP3 may contribute to preventing worsening of ventricular remodeling after myocarditis by depriving MMP2 activated by myocarditis-mediated ACE2 reduction of its abilities to degrade myocardial ECM and promote new synthesis of type I and III collagen (Fig. 8). Our data provide a new mechanistic insight into ventricular remodeling after myocarditis and shed new light on the EP4 receptor as a therapeutic target for preventing DCM after myocarditis.

In a previous study using cultured human aortic smooth muscle cells or human abdominal aortic aneurism tissue organ cultures containing smooth muscle cells and macrophages, EP4 stimulation with ONO-AE1-329 increased MMP2 activation, while ONO-AE3-208, an EP4 antagonist decreased its activation.[41] These observations were contrast to our results. However, in another study using cardiac

fibroblast, EP4 agonist reduced the activation of MMP2 and the expression of its key activator, MT1-MMP.[42] Moreover, aged mice lacking the EP4 receptor in cardiomyocytes display a phenotype of dilated cardiomyopathy coupled with increased expression of MMP2 as well as MT1-MMP in the left ventricle.[43] Stimulation of EP4 receptor may produce different phenotypes on different types of cells and organs.

Long-term administration of a high dose of EP4 selective agonist might lead to cardiac hypertrophy and dyslipidemia. In our *in vivo* experimental setting with healthy mice, continued administration of 50 mg/kg/day of ONO-0260164 for 49 days significantly increased LV mass index via increasing LV wall thickness rather than LV dimensions. Consistently, several reports have demonstrated that activation of EP4 receptor signaling contributes to the PGE2-mediated cardiac hypertrophy, which is characterized by larger cross-sectional area of cardiomyocytes.[44–45] Moreover, in our study, continued administration of the high dose also increased body weight, consistent with a previous report showing that animal models mice lacking EP4 exhibited slower weight gain and reduced adiposity upon high fat diet challenge when compared with wild type mice.[46] Since activation of PGE2-EP4 signaling can exert multiple biochemical effects including cardiac function and structure and lipid metabolism, setting the appropriate therapeutic dose for the diseases is very important.

In conclusion, the present study using EAM mice delineated for the first time that myocardial ECM metabolism by MMP2 activation is an important and novel molecular mechanism underlying adverse ventricular remodeling after myocarditis and that continued treatment with selective EP4 receptor stimulant rescues cardiac malfunction during myocarditis and exhibits robust preventive effects against adverse ventricular remodeling after myocarditis in association with the control of MMP2 activation. EP4 receptor stimulant could potentially become a part of new strategy to prevent heart failure caused by inflammatory heart disease.

Methods

Ethics Statement

All animal studies were approved by the Institutional Animal Care and Use Committees of Yokohama City University (license number: F-A-18-043) and carried out in accordance with the guidelines of Yokohama City University. Moreover, the present study was also carried out in compliance with the ARRIVE (Animal Research: Reporting of In Vivo Experiments) guidelines (https://arriveguidelines.org/arrive-guidelines).

Induction of EAM model

Six- to eight-week-old male BALB/cJ background mice (Jackson Laboratory) were subcutaneously immunized with 150 μg of myocarditogenic peptide (Alpha-Myosin Heavy Chain-MyHC-$\alpha_{614-634}$, Ac-SLKLMATLFSTYASAD-OH, AnaSpec, Belgium) emulsified 1:1 in PBS/complete Freund's adjuvant (CFA) (1 mg/ml, H37Ra; Difco) or PBS/CFA only on days 0 and 7.[47] Before immunization, all mice were

anesthetized with 2.0 Vol% isoflurane inhalation in oxygen. Myocarditis severity was evaluated by using a 0 to 4 scoring system.[47]

Treatment protocols

A EP4 selective agonist, ONO-0260164 was kindly provided by Ono Pharmaceutical Co., Ltd (Osaka, Japan).[15] A EP4 selective antagonist, CJ-42794 was purchased from Cayman Chemicals (Ann Arbor, MI, USA).

At 2 weeks after immunization with myosin/CFA/PBS, the EAM mice were randomly separated into subgroups and daily administered 20 mg/kg of ONO-0260164, 30 mg/kg of CJ-42794, or vehicle via gastric gavage from day 14 to day 21 and 56 according to treatment protocols as follows: (A) Either CJ-42794 or vehicle (0.5% methylcellulose) for 1 week (day 14 to 21); (B) Either ONO-0260164 or vehicle (water) for 6 weeks (day 14 to 56); (C) both ONO-0260164 and CJ-42794, ONO-0260164 only, or vehicle only (water / 0.5% methylcellulose) for 6 weeks (day 14 to 56). On the other hand, non-EAM mice were treated daily with vehicle only starting 2 weeks after immunization with CFA/PBS alone (day 14 to 21 or day 14 to 56). Apart from these protocols, to clarify the dose-dependent *in vivo* responses of normal mice to the drug, water, 2, 20, or 50 mg/kg of ONO-0260164 was administered to unimmunized healthy mice.

Echocardiographic measurements

Trans-thoracic echocardiography was performed with a Vevo 3100LT system (VisualSonics, Fujifilm, Tokyo, Japan) equipped with a MX400 20–46 MHz linear array transducer (Visual Sonics, Fujifilm, Tokyo, Japan) at 14, 21, and 56 days after immunization. The mice were anesthetized by 2.0 Vol% isoflurane inhalation in oxygen and were placed in a lateral position on a heating pad and chest hair was removed. Heart rate was monitored continuously during the examination. Hearts were imaged in the two-dimensional mode in short-axis views at the level of papillary muscle. M-mode views were used to measure the left ventricular (LV) dimensions according to the American Society for Echocardiography leading edge method [48], including LV end-diastolic dimension (LVDd), LV end-systolic dimension (LVDs), interventricular septum diastolic or systolic thickness (IVSd or IVSs), and LV posterior wall diastolic or systolic thickness (PWd or PWs). Fractional shortening (FS = [(LVDd − LVDs)/LVDd] × 100) and LV mass index (LVMI) [LV mass/body weight] = 1.04 [$(LVDd + PWd + IVSd)^3 - LVDd^3$] × 0.8 + 0.6 / g) were calculated with Vevolab software (VisualSonics version 3.2.0, Fujifilm, Tokyo, Japan). All echocardiographic examinations were performed by the same examiner blinded to the identity of the mouse.

Blood pressure measurement

Systolic blood pressure (BP) and heart rate (HR) were evaluated before and 1 and 2 hours after a single administration or after daily administration for 0, 21, or 49 days in healthy mice or evaluated at day 21 or 56 after immunization in EAM or non-EAM mice. The BP and HR were measured at the same time point in conscious mice by using a tail-cuff system (MK-2000; Muromachi Kikai Co., Tokyo, Japan). All examinations were performed by the same examiner blinded to the identity of the mouse.

Isolation and preservation of heart samples

Anesthetized mice were perfused with cold PBS until the liver turned whitish after blood (>700 μL) was collected. Subsequently, hearts were removed from the euthanized mice, and the isolated ventricles were stored at −80°C until protein and mRNA analyses. Alternatively, isolated ventricles for myocardial pathology were cut at the level of the papillary muscles and then harvested in 10% formalin solution. Anesthesia and euthanasia for all mouse experiments were performed by continuous inhalation of 5.0 Vol% isoflurane.

Pathology

We obtained transverse sections of paraffin-embedded heart (5 μm) for histopathological examination. To identify myocardial inflammation and collagen deposition, ventricular cross-sections, which were deparaffinized and subsequently rehydrated, were then stained with hematoxylin-eosin and picrosirius red, respectively. Collagen staining was performed according to *manufacturer* protocol (Picro-Sirius Red Stain Kit [For Cardiac Muscle], SRC-1, ScyTek Lab). Area of myocardial inflammation or collagen deposition was calculated as the area ratio (affected area / LV area × 100 %) using the Image J software. Values for three ventricular regions were averaged for each heart, and the mean percentage of affected area for each group was calculated. All data were analyzed in a blind fashion by two independent investigators and averaged.

Immunohistochemistry

Ventricular cross-sections of paraffin-embedded heart tissue, which were removed 21 days after immunization with cardiac myosin, were deparaffinized and rehydrated, and then endogenous peroxidase activity was blocked in 3% hydrogen peroxide in methanol for 10 minutes. After blocking with 2.5% BSA in PBS for 30 minutes, samples were incubated overnight at 4°C with primary anti-body for EP4 (1:100) (Santa Cruz Biotechnology, CA, USA) and then incubated at room temperature with the VECTASTAIN ABC Kit according to manufacturer protocol (Vector laboratories, CA, USA). Ultimately, EP4 signal was detected with streptavidin-peroxidase complex with diaminobenzidine. Negative control sections were incubated with secondary Ab alone.

RNA extraction, reverse transcription, and quantitative real-time PCR

RNA was isolated from heart tissues with Trizol Reagent (Invitrogen) according to the manufacturer's protocol. cDNA synthesis was performed using 2.0 μg RNA and PrimeScript RT reagent Kit (Takara, Tokyo, Japan). Quantitative real-time PCR was performed with TB Green Premix Ex Taq II (Takara, Tokyo, Japan) using a CFX96 Real-Time PCR Detection System (Bio-Rad), with GAPDH as internal control. Reactions were performed in 25-μL containing cDNA (2.0 μL), TB Green Premix Ex Taq II (2×, 12.5 μL), PCR forward Primer (10 μM, 1.0 μL), PCR reverse primer (10 μM, 1.0 μL), and ddH2O (8.5 μL). PCR was performed at 95°C for 30 sec, followed by 50 cycles of 95°C for 5 sec and 60°C for 30 sec. Gene expression was analyzed using the 2-ΔΔCt method. Target mRNA expression was compared as relative ratio to the housekeeping gene GAPDH. The sequences of the primers are shown in Supplementary Table 1.

Western blot analysis

Cardiac tissue homogenates were lysed in NP-40 with protease inhibitor. Proteins (25μg / well) were separated by SDS-PAGE, transferred to a nitrocellulose membrane, and incubated with primary antibodies to EP4 (Santa Cruz Biotechnology, CA, USA), tissue inhibitor of metalloproteinase (TIMP)-3 (Proteintech, IL, USA), and GAPDH (Cell Signaling Technology, MA, USA) at 4°C overnight. The membranes were then incubated with a secondary antibody (Cell Signaling Technology, MA, USA) for 1 hour at room temperature and developed with ECL reagent. Enhanced chemiluminescence was detected with an LAS-3000 (Fujifilm, Tokyo, Japan).

Gelatin Zymography

Proteolytic activity of cardiac tissue homogenates was examined by gelatin zymography according to the manufacturer's protocol (Cosmo Bio Co., Ltd., Tokyo, Japan). Samples (25μg / well) were subjected to 10% SDS–polyacrylamide gel electrophoresis using gels containing 0.1% gelatin. Gels were incubated at 37°C for 24 hours in enzyme reaction buffer and then stained with 0.5% Coomassie Brilliant Blue R-250 in 50% methanol and 10% acetic acid for 1 h. MMP marker (Cosmo Bio Co., Ltd.) was used as a matrix metalloproteinase marker. The proteolytic bands of 62, 66, and 92kDa corresponding to the active form of MMP-2, ProMMP-2, and ProMMP-9, respectively were scanned using a Photo scanner.

Statistical analysis

Comparisons between the 2 groups with the different treatment were performed by the nonparametric 2-tailed Mann-Whitney test. Data from different time points or different treatments were analyzed with 2-way ANOVA followed by the Bonferroni-Dunn post hoc testing method. All experiments were performed

independently at least three times. All data were analyzed in a blind fashion by two independent investigators and averaged. All data are presented as dot and box plots or mean±SEM. A P value less than 0.05 was considered significant. Data analyses were done using the JMP ver. 12.2 software.

Declarations

Acknowledgments

We gratefully thank Ono Pharmaceutical Co., Ltd for providing the ONO-0260164. This work was supported by Grant-in-Aid for Scientific Research (grant number 19K09401) and YOKOHMA ACADEMIC FOUNDATION.

Author Contributions

1. Dr A Takakuma performed all experiments and acquired the data. 2. Dr M Nishii conceived and designed the research, edited the whole manuscript, and drafted the manuscript. 3. Dr A Valaperti helped a critical part of experiments and made critical revision of the manuscript for key intellectual content. 4. Drs R Saji, H Hiraga, K Sakai, R Matsumura, Y Miyata, N Oba, F Nunose, F Ogawa helped a part of experiments. 5. Professor Drs K Tamura and I takeuchi supervised this work.

Competing Interests Statement:

none

References

1. McCarthy, R. E. *et al.* Long-term outcome of fulminant myocarditis as compared with acute (nonfulminant) myocarditis. *N. Engl. J. Med*, **342**, 690–695 (2000).
2. Ammirati, E. *et al.* Survival and left ventricular function changes in fulminant versus nonfulminant acute myocarditis. *Circulation*, **136**, 529–545 (2017).
3. Jin, O. *et al.* Detection of enterovirus RNA in myocardial biopsies from patients with myocarditis and cardiomyopathy using gene amplification by polymerase chain reaction. *Circulation*, **82**, 8–16 (1990).
4. Hühl, U., Noutsias, M., Seeberg, B. & Schultheiss, H. P. Immunohistochemical evidence for a chronic intramyocardial inflammatory process in dilated cardiomyopathy. *Heart*, **75**, 295–300 (1996).
5. Lauer, B., Padberg, K., Schultheiss, H. P. & Strauer, B. E. Autoantibodies against cardiac myosin in patients with myocarditis and dilated cardiomyopathy. *Z. Kardiol*, **84**, 301–310 (1995).
6. Li, J. *et al.* Collagen degradation in a murine myocarditis model: relevance of matrix metalloproteinase in association with inflammatory induction. *Cardiovasc. Res*, **56**, 235–247 (2002).

7. Woodiwiss, A. J. *et al.* Reduction in myocardial collagen cross-linking parallels left ventricular dilatation in rat models of systolic chamber dysfunction. *Circulation*, **103**, 155–160 (2001).
8. Kong, P., Christia, P. & Frangogiannis, N. G. The Pathogenesis of Cardiac Fibrosis. *Cell. Mol. Life. Sci*, **71**, 549–574 (2014).
9. Conrad, C. H. *et al.* Myocardial fibrosis and stiffness with hypertrophy and heart failure in the spontaneously hypertensive rat. *Circulation*, **91**, 161–170 (1995).
10. Janicki, J. S. & Brower, G. L. The role of myocardial fibrillar collagen in ventricular remodeling and function. *J. Card. Fail*, **8**, 319–325 (2002).
11. Harris, S. G., Padilla, J., Koumas, L., Ray, D. & Phipps, R. P. Prostaglandins as modulators of immunity. *Trends. Immunol*, **23**, 144–150 (2002).
12. Xiao, C. Y. *et al.* Prostaglandin E2 protects the heart from ischemia-reperfusion injury via its receptor subtype EP4. *Circulation*, **109**, 2462–2468 (2004).
13. Bryson, T. D. *et al.* Overexpression of prostaglandin E2 EP4 receptor improves cardiac function after myocardial infarction. *J. Mol. Cell. Cardiol*, **118**, 1–12 (2018).
14. Hishikari, K. *et al.* Pharmacological activation of the prostaglandin E2 receptor EP4 improves cardiac function after myocardial ischaemia/reperfusion injury. *Cardiovasc. Res*, **81**, 123–132 (2009).
15. Wang, Q. *et al.* An EP4 Receptor Agonist Inhibits Cardiac Fibrosis Through Activation of PKA Signaling in Hypertrophied Heart. *Int. Heart. J*, **58**, 107–114 (2017).
16. Błyszczuk, P. Myocarditis in Humans and in Experimental Animal Models. *Front. Cardiovasc. Med*, **6**, 64 (2019).
17. Ngoc, P. B. *et al.* The anti-inflammatory mechanism of prostaglandin e2 receptor 4 activation in rat experimental autoimmune myocarditis. *J. Cardiovasc. Pharmacol*, **57**, 365–372 (2011).
18. Yamashita, T. *et al.* IL-6-mediated Th17 differentiation through RORγt is essential for the initiation of experimental autoimmune myocarditis. *Cardiovasc. Res*, **91**, 640–648 (2011).
19. Kania, G., Blyszczuk, P. & Eriksson, U. Mechanisms of cardiac fibrosis in inflammatory heart disease. *Trends. Cardiovasc. Med*, **19**, 247–252 (2009).
20. Matsumura, S. *et al.* Targeted deletion or pharmacological inhibition of MMP-2 prevents cardiac rupture after myocardial infarction in mice. *J. Clin. Invest*, **115**, 599–609 (2005).
21. Bergman, M. R. *et al.* Cardiac matrix metalloproteinase-2 expression independently induces marked ventricular remodeling and systolic dysfunction. *Am. J. Physiol. Heart. Circ. Physiol*, **292**, 1847–1860 (2007).
22. Bujak, M. & Frangogiannis, N. G. The role of TGF-beta signaling in myocardial infarction and cardiac remodeling. *Cardiovasc. Res*, **74**, 184–195 (2007).
23. Cohen, L. *et al.* Cardiac remodeling secondary to chronic volume overload is attenuated by a novel MMP9/2 blocking antibody. *PLoS. One*, **15**, e0231202 (2020).
24. Mehta, P. K. & Griendling, K. K. Angiotensin II cell signaling: Physiological and pathological effects in the cardiovascular system. *Am. J. Physiol. Cell. Physiol*, **292**, C82–C97 (2007).

25. Crackower, M. A. *et al.* Angiotensin-converting enzyme 2 is an essential regulator of heart function. *Nature*, **417**, 822–828 (2002).
26. Zhong, J. *et al.* Angiotensin-converting enzyme 2 suppresses pathological hypertrophy, myocardial fibrosis, and cardiac dysfunction. *Circulation*, **122**, 717–728 (2010).
27. Brower, G. L., Levick, S. P. & Janicki, J. S. Inhibition of matrix metalloproteinase activity by ACE inhibitors prevents left ventricular remodeling in a rat model of heart failure. *Am. J. Physiol. Heart. Circ. Physiol*, **292**, H3057–3064 (2007).
28. Kassiri, Z. *et al.* Loss of angiotensin-converting enzyme 2 accelerates maladaptive left ventricular remodeling in response to myocardial infarction. *Circ. Heart. Fail*, **2**, 446–455 (2009).
29. Wang, Z., Juttermann, R. & Soloway, P. D. TIMP-2 is required for efficient activation of proMMP-2 in vivo. *J. Biol. Chem*, **275**, 26411–26415 (2000).
30. Li, Y. Y., McTiernan, C. F. & Feldman, A. M. Interplay of matrix metalloproteinases, tissue inhibitors of metalloproteinases and their regulators in cardiac matrix remodeling. *Cardiovasc. Res*, **46**, 214–224 (2000).
31. Spinale, F. G. Myocardial matrix remodeling and the matrix metalloproteinases: influence on cardiac form and function. *Physiol. Rev*, **87**, 1285–1342 (2007).
32. Maquart, F. X. *et al.* Stimulation of collagen synthesis in fibroblast cultures by the tripeptide-copper complex glycyl-L-histidyl-L-lysine-Cu2+. *FEBS. Lett*, **238**, 343–346 (1988).
33. Polyakova, V. *et al.* Fibrosis in endstage human heart failure: severe changes in collagen metabolism and MMP/TIMP profiles. *Int. J. Cardiol*, **151**, 18–33 (2011).
34. Nagaoka, I. & Hirota, S. Increased expression of matrix metalloproteinase-9 in neutrophils in glycogen-induced peritoneal inflammation of guinea pigs. *Inflamm. Res*, **49**, 55–62 (2000).
35. Tao, Z. Y., Cavasin, M. A., Yang, F., Liu, Y. H. & Yang, X. P. Temporal changes in matrix metalloproteinase expression and inflammatory response associated with cardiac rupture after myocardial infarction in mice. *Life. Sci*, **74**, 1561–1572 (2004).
36. Yao, C. *et al.* Prostaglandin E2-EP4 signaling promotes immune inflammation through Th1 cell differentiation and Th17 cell expansion. *Nat. Med*, **15**, 633–640 (2009).
37. Esaki, Y. Dual roles of PGE2-EP4 signaling in mouse experimental autoimmune encephalomyelitis. Proc. Natl. Acad. Sci. U S A. 107, 12233–12238(2010).
38. Knäuper., V. *et al.* Cellular mechanisms for human procollagenase-3 (MMP-13) activation. Evidence that MT1-MMP (MMP-14) and gelatinase a (MMP-2) are able to generate active enzyme. *J. Biol. Chem*, **271**, 17124–17131 (1996).
39. Kassiri, Z. *et al.* Combination of tumor necrosis factor-alpha ablation and matrix metalloproteinase inhibition prevents heart failure after pressure overload in tissue inhibitor of metalloproteinase-3 knock-out mice. *Circ. Res*, **97**, 380–390 (2005).
40. Koskivirta, I. *et al.* Mice with tissue inhibitor of metalloproteinases 4 (Timp4) deletion succumb to induced myocardial infarction but not to cardiac pressure overload. *J. Biol. Chem*, **285**, 24487–

24493 (2010).

41. Yokoyama, U. *et al.* Inhibition of EP4 signaling attenuates aortic aneurysm formation. *PLoS. One*, **7**, e36724 (2012).
42. Kassem, K. M., Clevenger, M. H., Szandzik, D. L., Peterson, E. & Harding, P. PGE2 reduces MMP-14 and increases plasminogen activator inhibitor-1 in cardiac fibroblasts. *Prostaglandins. Other. Lipid. Mediat*, **113**, 62–68 (2014).
43. Harding, P. *et al.* Gene expression profiling of dilated cardiomyopathy in older male EP4 knockout mice. *Am. J. Physiol. Heart. Circ. Physiol*, **298**, H623–32 (2010).
44. Qian, J. Y., Leung, A., Harding, P. & LaPointe, M. C. PGE2 stimulates human brain natriuretic peptide expression via EP4 and p42/44 MAPK. *Am. J. Physiol. Heart. Circ. Physiol*, **290**, H1740–1746 (2006).
45. He, Q., Harding, P., LaPointe, M. C. & PKA Rap1, ERK1/2, and p90RSK mediate PGE2 and EP4 signaling in neonatal ventricular myocytes. *Am. J. Physiol. Heart. Circ. Physiol*, **298**, H136–143 (2010).
46. Cai, Y. *et al.* Mice lacking prostaglandin E receptor subtype 4 manifest disrupted lipid metabolism attributable to impaired triglyceride clearance. *The. FASEB. Journal*, **29**, 4924–4936 (2015).
47. Valaperti, A. *et al.* CD11b + monocytes abrogate Th17 CD4 + T cell-mediated experimental autoimmune myocarditis. *J. Immunol*, **180**, 2686–2695 (2008).
48. Litwin, S. E., Katz, S. E., Morgan, J. P. & Douglas, P. S. Serial echocardiographic assessment of left ventricular geometry and function after large myocardial infarction in the rat. *Circulation*, **89**, 345–354 (1994).

Figures

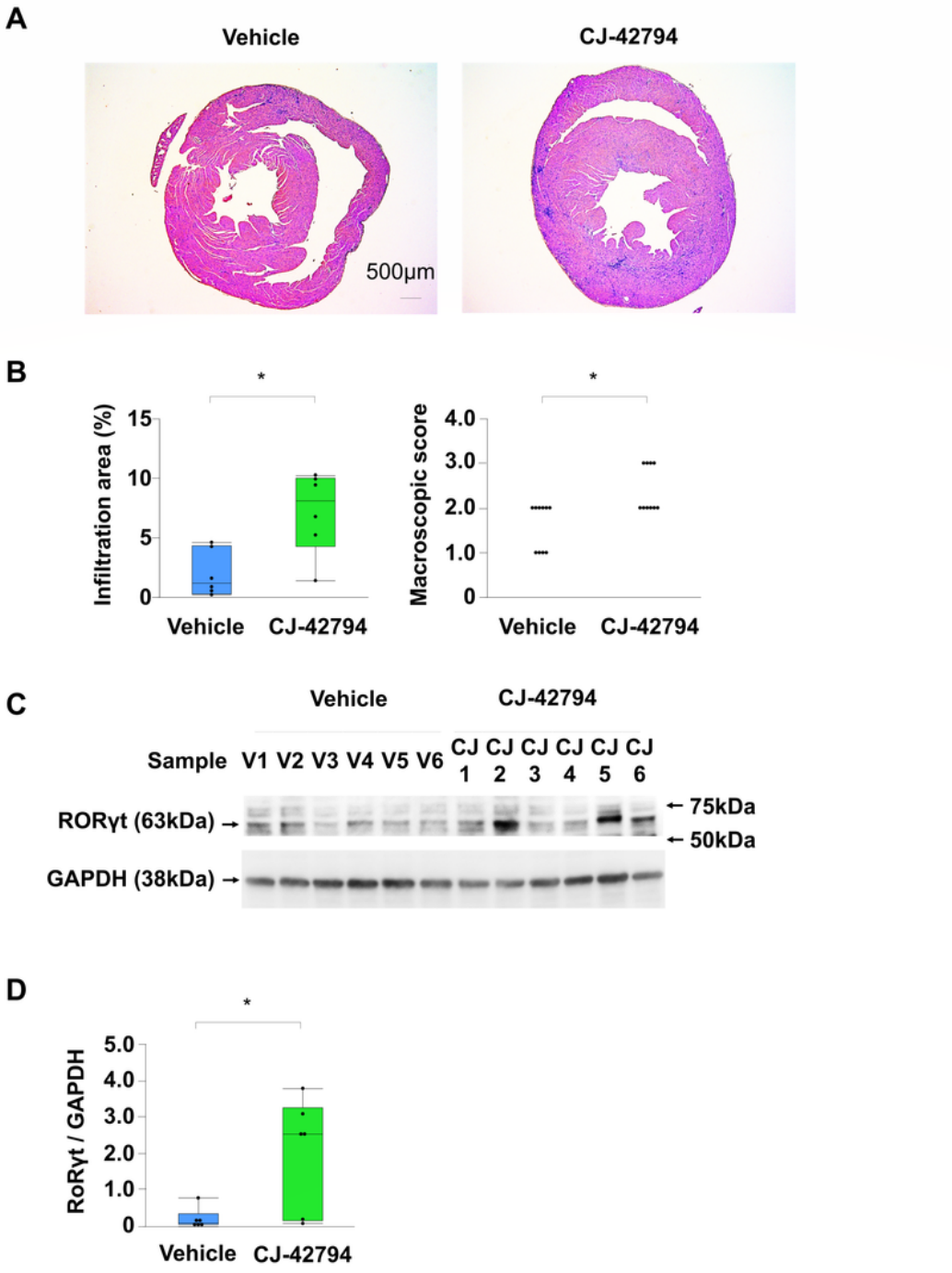

Figure 1

Myocardial inflammation in the experimental autoimmune myocarditis (EAM). (A) Representative Hematoxylin-Eosin staining and (B) statistical analyses of inflamed area (n=6 / each) and macroscopic score (n=10 / each) in ventricular cross-sections and hearts, respectively on day 21 obtained from EAM treated daily with vehicle or selective prostaglandin E2 receptor 4 (EP4) antagonist (CJ-42794) from day 14 to day 21. Scale bars: 500 μm. Inflamed area was calculated by affected area / ventricular area × 100

%. (C) Western blot (cropped gel) and (D) its densitometric analysis (n=6 / each) of the EAM inducible Th17-specific master transcription factor, retinoic acid receptor-related orphan nuclear receptor (ROR γt) on day 21 hearts from EAM mice treated with vehicle or CJ-42794. Full-length blots of ROR γt and GAPDH are presented in Supplementary Figure 6A. P* < 0.05 (vs. vehicle) calculated with nonparametric 2-tailed Mann-Whitney U test.

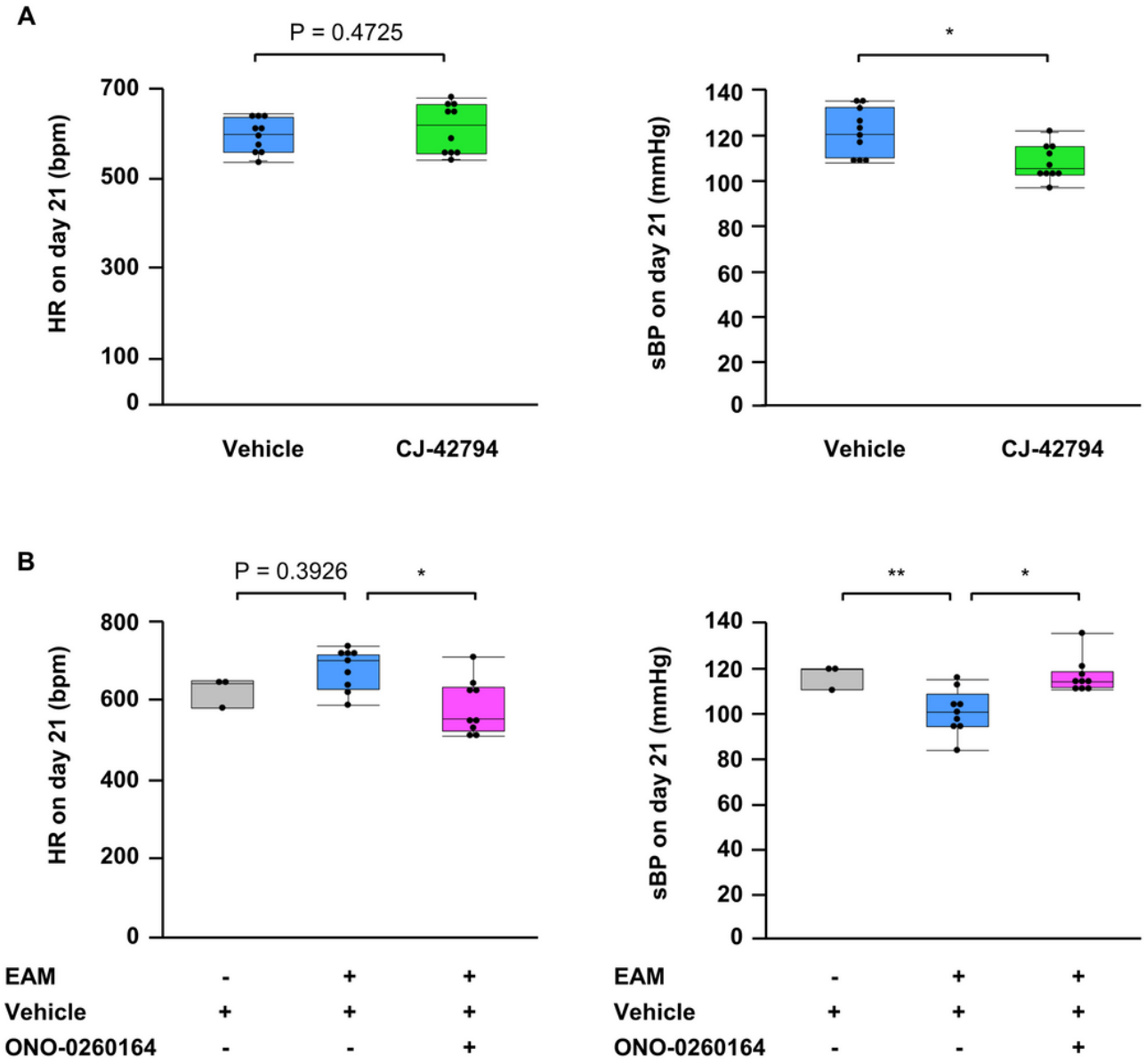

Figure 2

Systolic blood pressure (BP) and heart rate (HR) in experimental autoimmune myocarditis (EAM) mice. (A) HR and BP on day 21 in EAM mice daily treated with vehicle (n=10) or selective prostaglandin E2 receptor 4 (EP4) antagonist (CJ-42794) (n=10) from day 14 to day 21. (B) HR and BP on day 21 in non-EAM mice daily treated with vehicle (n=5) or in EAM mice daily treated with vehicle only (n=9) or selective EP4 agonist (ONO-0260164) (n=9) from day 14 to day 21. (A) P* < 0.05 (vs. vehicle alone-treated EAM)

calculated with nonparametric 2-tailed Mann-Whitney U test. (B) P* < 0.05 (vs. vehicle alone-treated EAM) or P** < 0.05 (vs. non-EAM) calculated with 2-way ANOVA followed by the Bonferroni-Dunn post hoc testing method.

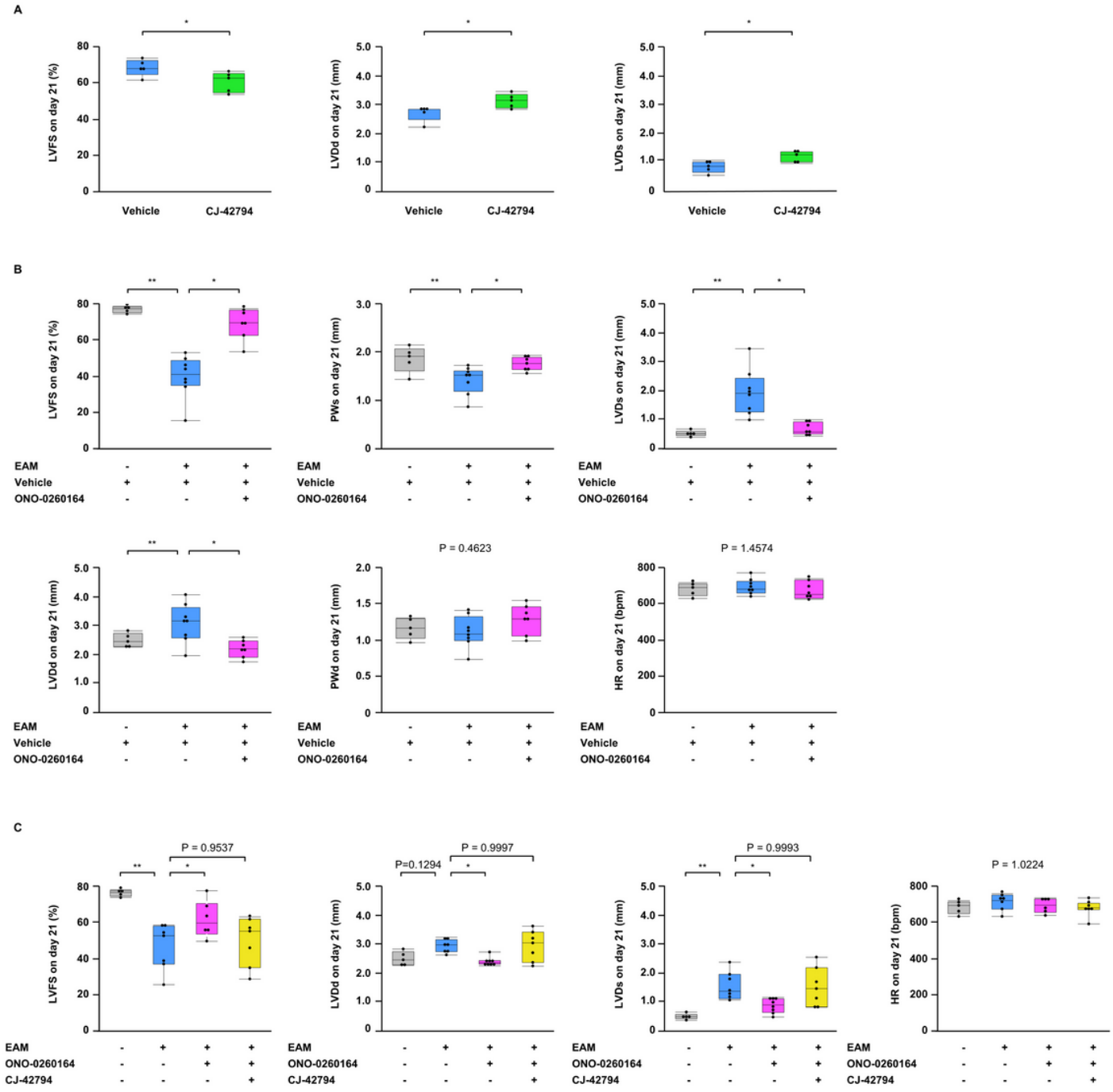

Figure 3

Cardiac malfunction in experimental autoimmune myocarditis (EAM) mice. (A) Echocardiographic findings on day 21 in EAM mice daily treated with vehicle or selective prostaglandin E2 receptor 4 (EP4) antagonist (CJ-42794) from day 14 to day 21 (n=5 / each). (B) Echocardiographic findings on day 21 in

non-EAM mice daily treated with vehicle only (n=5) or in EAM mice treated with vehicle (n=8) or selective EP4 agonist (ONO-0260164) (n=7) from day 14 to day 21. (C) Echocardiographic findings on day 21 in non-EAM mice daily treated with vehicle only (n=5) or in EAM mice daily treated with vehicle (n=7), ONO-0260164 (n=6), or both ONO-0260164 and CJ-42794 (n=7) from day 14 to day 21. LVFS: Left ventricular fractional shortening; PWd or PWs: LV posterior wall diastolic or systolic thickness, respectively; LVDd: LV end-diastolic dimension; LVDs: LV end-systolic dimension; HR: Heart rate. (A) P* < 0.05 (vs. vehicle alone-treated EAM) calculated with nonparametric 2-tailed Mann-Whitney U test. (B-C) P* < 0.05 (vs. vehicle alone-treated EAM) or P** < 0.05 (vs. non-EAM) calculated with 2-way ANOVA followed by the Bonferroni-Dunn post hoc testing method.

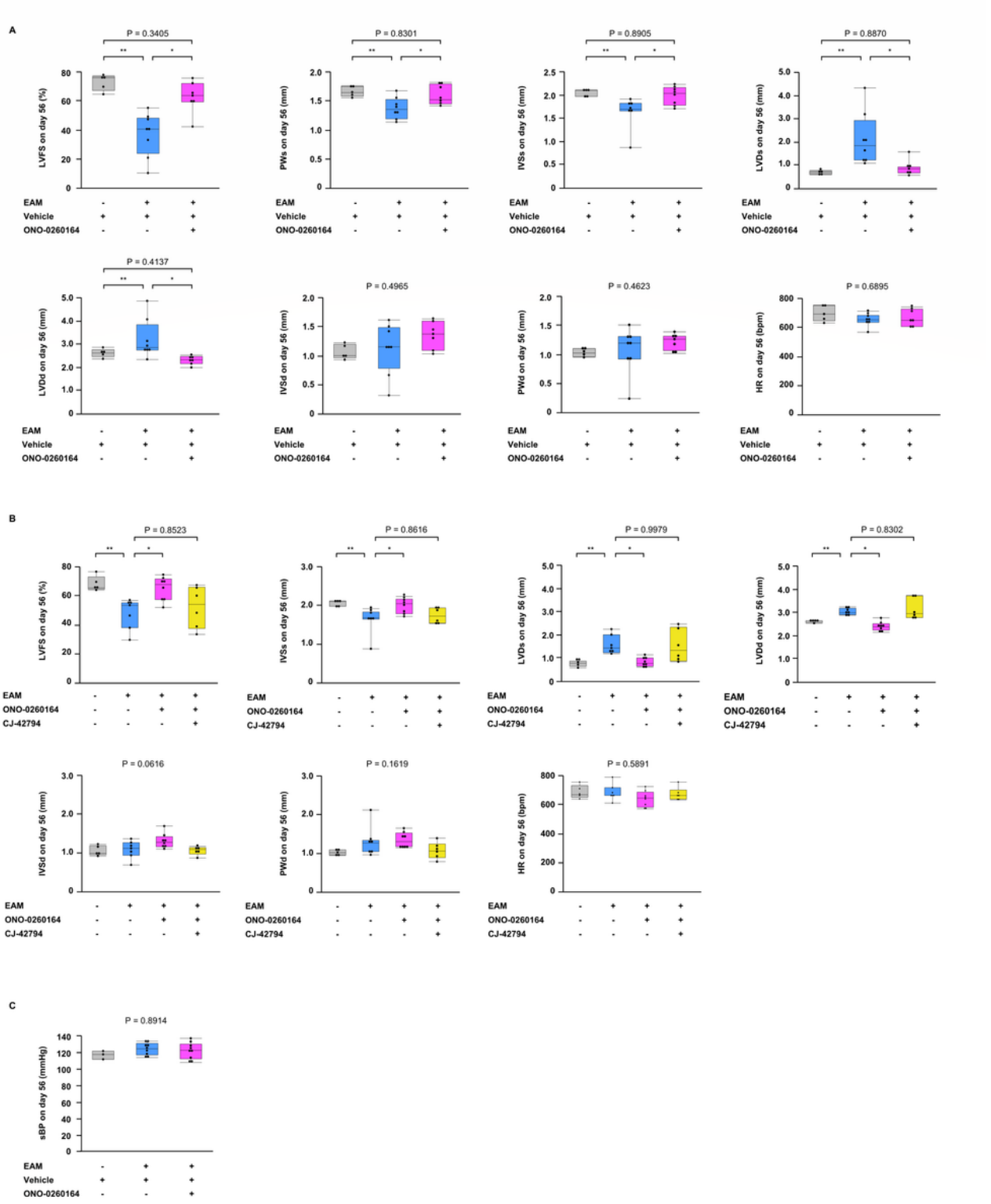

Figure 4

Dilated cardiomyopathy phenotype in experimental autoimmune myocarditis (EAM) mice. (A) Echocardiographic findings on day 56 in non-EAM mice treated daily with vehicle only (n=5) or in EAM mice treated daily with vehicle (n=8) or selective prostaglandin E2 receptor 4 (EP4) agonist (ONO-0260164) (n=7) from day 14 to day 56. (B) Echocardiographic findings on day 56 in non-EAM mice treated daily with vehicle only (n=5) or in EAM mice treated daily with vehicle (n=7), ONO-0260164 (n=8),

or both ONO-0260164 and selective EP4 antagonist (CJ-42794) (n=6) from day 14 to day 56. (C) Systolic blood pressure (BP) on day 56 in non-EAM (n=3) or in the EAM daily treated with vehicle (n=9) or ONO-0260164 (n=9) from day 14 to day 56. LVFS: Left ventricular fractional shortening; IVSd or IVSs: Interventricular septum diastolic or systolic thickness, respectively; PWd or PWs: LV posterior wall diastolic or systolic thickness, respectively; LVDd: LV end-diastolic dimension; LVDs: LV end-systolic dimension; HR: Heart rate. P* < 0.05 (vs. vehicle alone-treated EAM) or P** < 0.05 (vs. non-EAM) calculated with 2-way ANOVA followed by the Bonferroni-Dunn post hoc testing method.

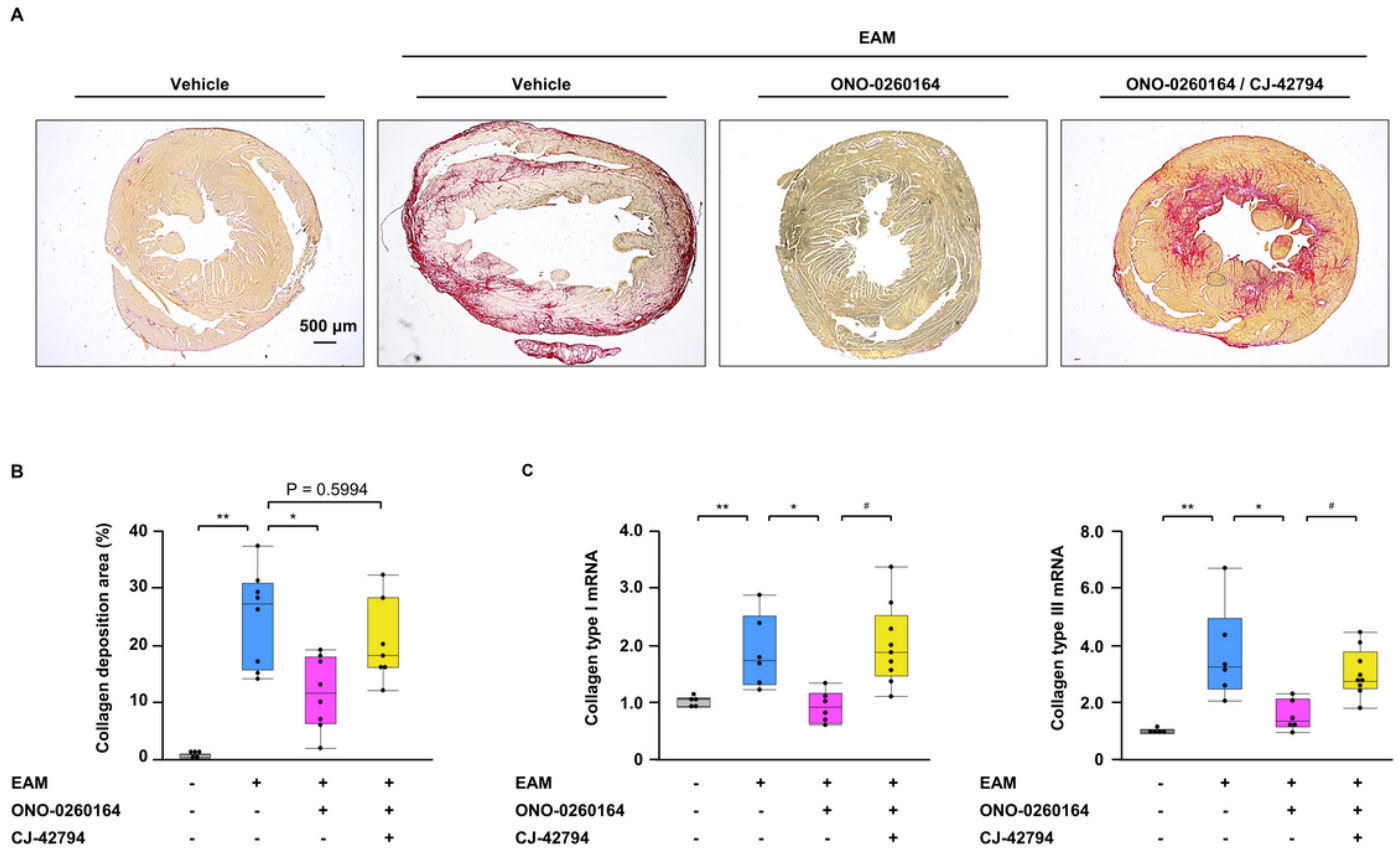

Figure 5

Myocardial collagen deposition in the experimental autoimmune myocarditis (EAM) mice. (A) Representative picrosirius red staining and (B) statistical analyses of collagen deposition area in ventricular cross-sections on day 56 obtained from non-EAM mice treated daily with vehicle (n=5) or from EAM mice treated daily with vehicle (n=8), selective prostaglandin E2 receptor 4 (EP4) agonist (ONO-0260164) (n=8), or both ONO-0260164 and selective EP4 antagonist (CJ-42794) (n=7) starting on day 14. Scale bars: 500 μm. Collagen deposition area was calculated by affected area / ventricular area × 100 %. (C) Reverse transcription-quantitative PCR for gene expression of collagen type I and type III in bulk heart tissues on day 56 obtained from non-EAM mice (n=5) or from EAM mice treated daily with vehicle (n=6), ONO-0260164 (n=6), or both CJ-42794 and ONO-0260164 (n=9). P* < 0.05 (vs. vehicle alone-treated EAM)

or P** < 0.05 (vs. non-EAM) or P# < 0.05 (vs. both CJ-42794 and ONO-0260164-treated EAM) calculated with 2-way ANOVA followed by the Bonferroni-Dunn post hoc testing method.

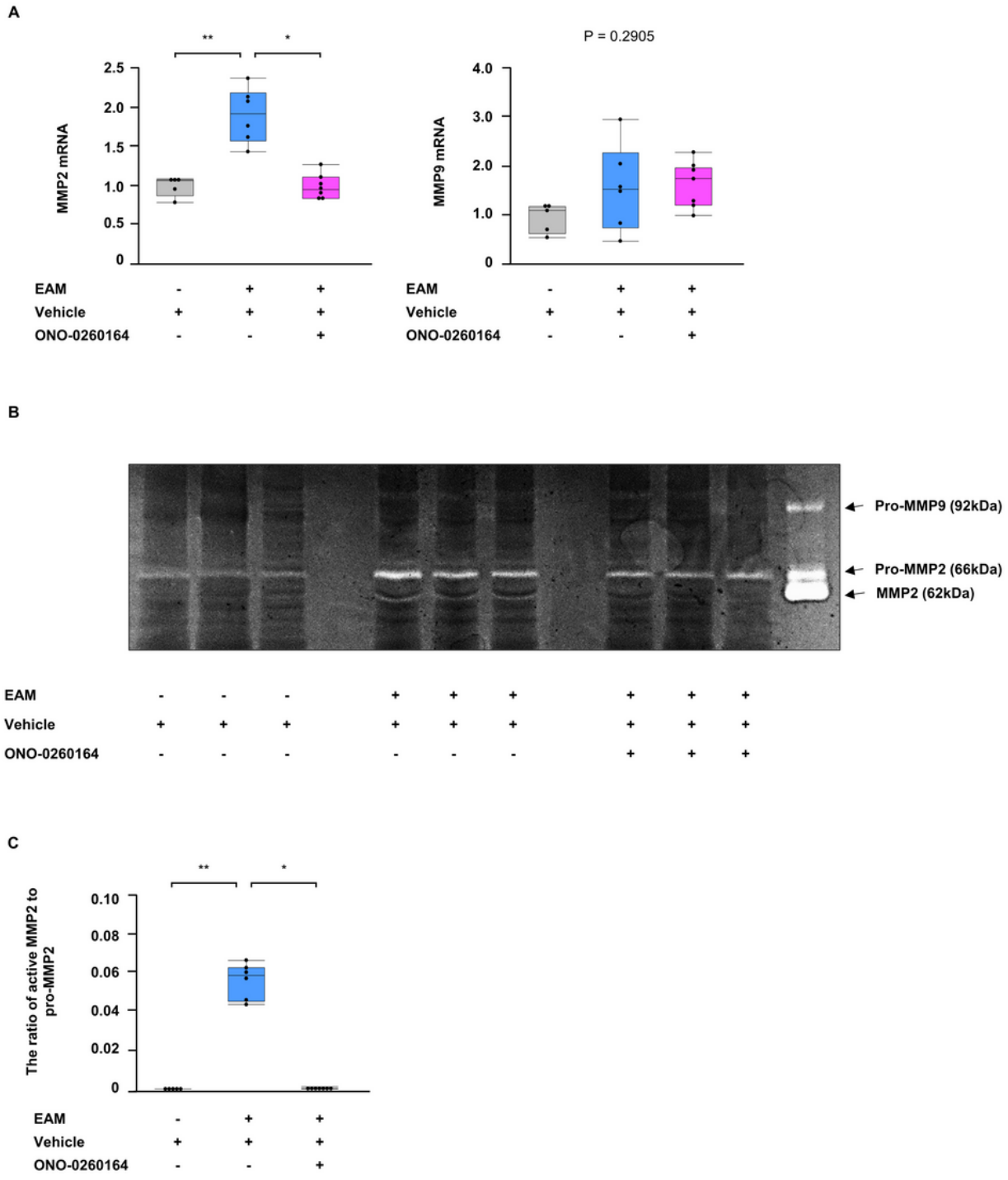

Figure 6

Expression and activation of matrix metalloproteinases (MMPs) in the heart of experimental autoimmune myocarditis (EAM) mice. (A) Reverse transcription-quantitative PCR, (B) representative gelatin zymography (cropped gel), and (C) densitometric analysis of MMPs including MMP2 and MMP9 in bulk

heart tissues on day 56 obtained from non-EAM mice treated daily with vehicle (n=5) or from EAM mice treated daily with vehicle (n=6) or selective prostaglandin E2 receptor 4 (EP4) agonist (ONO-0260164) (n=7) starting on day 14. The proteolytic bands of 62, 66, and 92kDa corresponding to the active form of MMP-2, ProMMP-2, and ProMMP-9, respectively were scanned using a Photo scanner. Full-length gel of MMP-2 and -9 is presented in Supplementary Figure 6B. P* < 0.05 (vs. vehicle alone-treated EAM) or P** < 0.05 (vs. non-EAM) calculated with 2-way ANOVA followed by the Bonferroni-Dunn post hoc testing method.

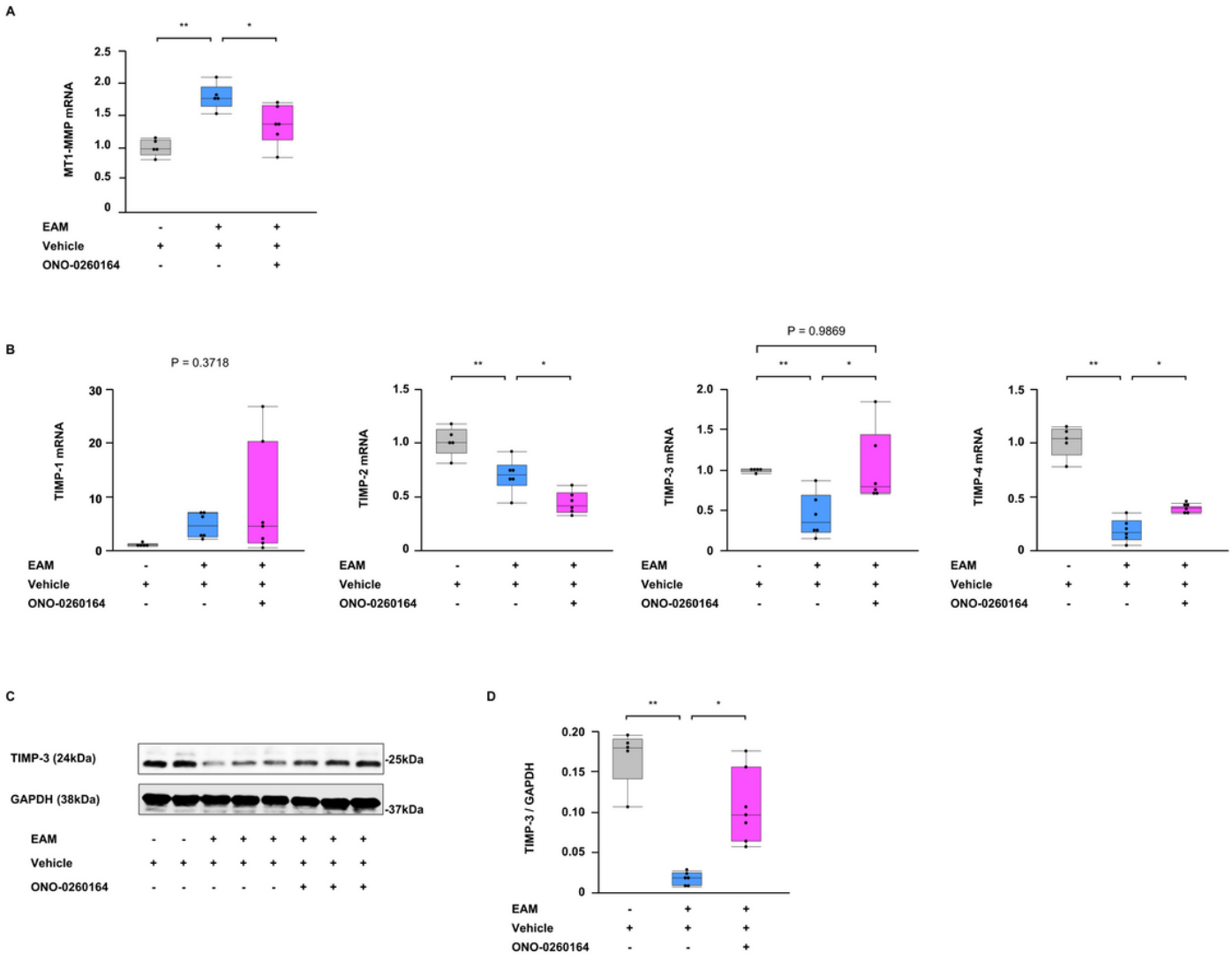

Figure 7

Endogenous regulators of matrix metalloproteinase (MMP) in the heart of experimental autoimmune myocarditis (EAM) mice. (A-B) Reverse transcription-quantitative PCR for membrane type (MT)-1 MMP and tissue inhibitors of metalloproteinases (TIMPs) and (C) representative western blot (cropped blot) and (D) densitometric analysis of theTIMP-3 in bulk heart tissues on day 56 obtained from non-EAM mice treated daily with vehicle (n=5) or from EAM mice treated daily with vehicle (n=6) or selective

prostaglandin E2 receptor 4 (EP4) agonist (ONO-0260164) (n=7) starting on day 14. Full-length blots of TIMP-3 and GAPDH are presented in Supplementary Figure 6C. P* < 0.05 (vs. vehicle alone-treated EAM) or P** < 0.05 (vs. non-EAM) calculated with 2-way ANOVA followed by the Bonferroni-Dunn post hoc testing method.

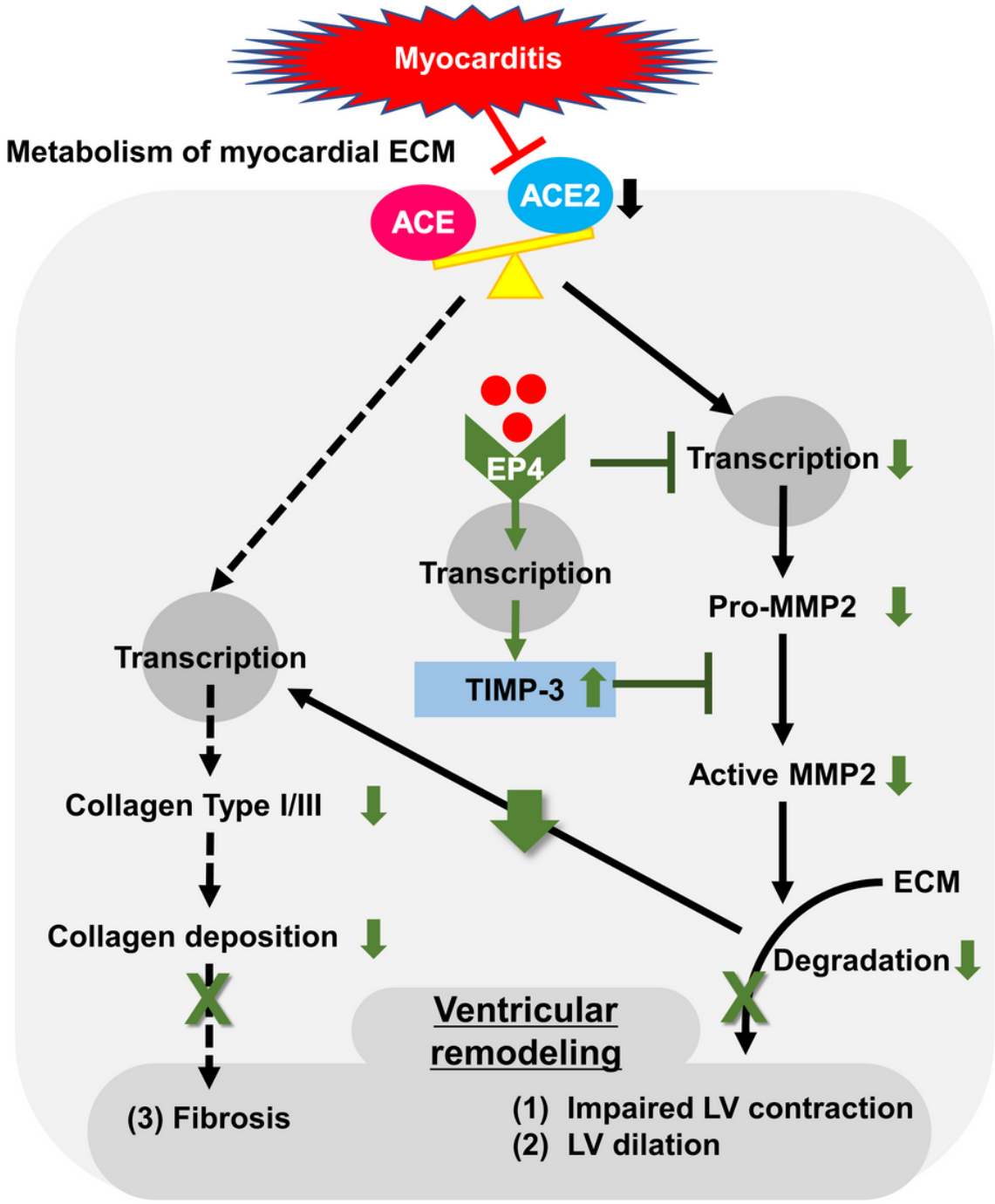

Figure 8

Schematic model illustrating the molecular mechanism for regulation of ventricular remodeling after myocarditis by prostaglandin E2 receptor 4 (EP4) stimulant. ACE: angiotensin-converting enzyme; MMP: matrix metalloproteinase; TIMP: tissue inhibitor of metalloproteinase; ECM: extracellular matrix; Red circles: ONO-0260164, a selective EP4 stimulant.

Supplementary Files

This is a list of supplementary files associated with this preprint. Click to download.

- Scientificreportsupplementnew2.pdf
- ScientificreportsupplemtaryVideo1.docx
- ScientificreportsupplemtaryVideo2.docx